ResearchGate

See discussions, stats, and author profiles for this publication at: https://www.researchgate.net/publication/320120829

Towards a wearable hand exoskeleton with embedded synergies

Conference Paper *in* Conference proceedings: ... Annual International Conference of the IEEE Engineering in Medicine and Biology Society. IEEE Engineering in Medicine and Biology Society. Conference · July 2017

DOI: 10.1109/EMBC.2017.8036800

CITATIONS
10

READS
483

4 authors, including:

Martin Burns
Stevens Institute of Technology
19 PUBLICATIONS **114** CITATIONS
SEE PROFILE

Vrajeshri Patel
Naval Health Research Center
13 PUBLICATIONS **107** CITATIONS
SEE PROFILE

Ramana Vinjamuri
University of Maryland, Baltimore County
58 PUBLICATIONS **978** CITATIONS
SEE PROFILE

Some of the authors of this publication are also working on these related projects:

hand synergies in prosthetics View project

All content following this page was uploaded by Ramana Vinjamuri on 12 December 2017.

The user has requested enhancement of the downloaded file.

Towards a wearable hand exoskeleton with embedded synergies

Martin K Burns, Katie Van Orden, Vrajeshri Patel, Ramana Vinjamuri, *Senior Member, IEEE*

***Abstract*— Numerous hand exoskeletons have been proposed in the literature with the aim of assisting or rehabilitating victims of stroke, brain/spinal cord injury, or other causes of hand paralysis. In this paper a new 3D printed soft hand exoskeleton, HEXOES (Hand Exoskeleton with Embedded Synergies), is introduced and mechanically characterized. Metacarpophalangeal (MCP) and proximal interphalangeal/ interphalangeal (PIP/IP) joints had measured maximum flexion angles of 53.7 ± 16.9° and 39.9 ± 13.4°, respectively; and maximum MCP and PIP angular velocities of 94.5 ± 41.9 degrees/s and 74.6 ± 67.3 degrees/s, respectively. These estimates indicate that the mechanical design has range of motion and angular velocity characteristics that meet the requirements for synergy-based control. When coupled with the proposed control loop, HEXOES can be used in the future as a test-bed for synergy-based clinical hand rehabilitation.**

I. Introduction

Individuals can lose the ability to perform activities of dialing living (ADL) independently as a result of stroke, spinal cord injury, or other neurological disorders. These individuals may then need to go through complicated and tedious physical therapy to restore function to their injured hand, or may be constrained to living with their impairment if the damage is irreparable. Repetitive extension and flexion therapy has been shown to improve grasping and releasing function, but is only effective when performed properly and often [1] [2]. In recent years, robotic exoskeleton devices have become popular candidates for performing these therapies in the future. These devices have been shown to improve the lives of those living with hand impairments by assisting in rehabilitation exercises or helping the user complete ADL that they may not otherwise be able to perform [3] [4]. These exoskeleton designs vary greatly in methods of actuation, degrees of freedom (DoF) and range of motion, but all aim to restore function to the user's impaired hand in some form.

Numerous unique active exoskeletons exist in the research phase with a wide variety of designs and control methods. Some devices, such as HEXORR, utilize electric actuators to drive gear trains or tendon mechanisms to flex and extend the fingers [5]. Other systems utilize pneumatic actuators, such as HWARD and the device created by Koeneman et al [8] [9]. Almost all of these devices along with numerous others utilize an EMG sensor system to track the intended movement of the user and guide their fingers to the correct position [10][11].

Research supported by the Center for Healthcare Innovation

Authors are with the Department of Biomedical Engineering, Chemistry, and Biological Sciences, Stevens Institute of Technology, Hoboken, NJ, USA (corresponding author phone: 201-216-3503; fax: 201-216-3531; e-mail: ramana.vinjamuri@stevens.edu).

In this paper the mechanical design of HEXOES, Hand Exoskeleton with Embedded Synergies, is presented along with preliminary kinematic characteristics from mannequin hand experiments. HEXOES is a tendon-driven soft glove-based exoskeleton which uses two motors per finger to actuate flexion and extension, resulting in a 5-DoF system. Future work is laid out to improve both the exoskeleton design and control system.

II. Exoskeleton Design

The HEXOES system is comprised of three subassemblies: the soft hand assembly, the hard motor assembly, and the mounting hardware. Fig. 1(a) shows a diagram outlining the layout of the two motors which control flexion and extension for a given finger while Fig. 1(b) shows the actual exoskeleton with major assemblies labeled. The mounting hardware consists of an orthopedic brace that has been modified to enable HEXOES to be mounted on an experimental rig for rehabilitation exercises or future robotic systems that implement the upper arm. The total mass of HEXOES is 1.134 kg.

A. Hand Assembly

The hand assembly is divided into four sections: sensors, finger components, palm guides and hand support.

The flex sensors (Tactilus Flex, Sensor Products Incorporated, Madison, NJ, USA) embedded in HEXOES produce a variable resistance based on the degree they are bent to. The hand assembly utilizes ten sensors stitched into the back of the glove to measure the angles of the MCP and

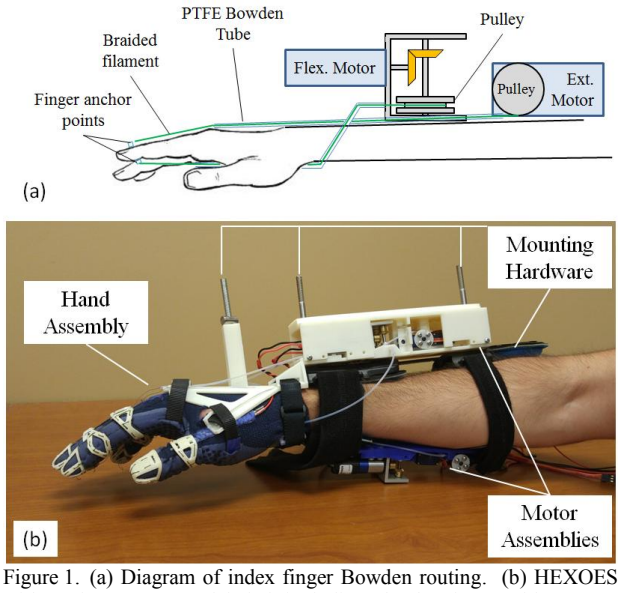

Figure 1. (a) Diagram of index finger Bowden routing. (b) HEXOES with major structures labeled including the hand assembly, motor assembly, and mounting hardware.

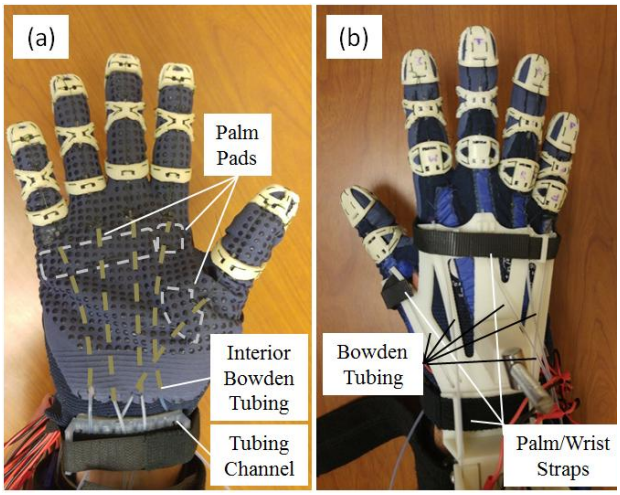

Figure 2. (a) Palmar view of hand assembly highlighting interior Bowden tubing and 3D printed palm pads. (b) Dorsal view of hand assembly showing the backplate, hook-and-loop straps, and extension bowden tubing

PIP/IP joint of the thumb and fingers of the hand. The varying resistance output from the sensors is converted to a varying voltage using voltage dividers, digitized by an Arduino microcontroller, and filtered using a third-order low-pass Butterworth filter with a 1.5 Hz cutoff frequency. These filtered voltages are then calibrated into joint angles using a linear approximation based on goniometer measurements taken with each finger in either full flexion or full extension.

The finger components serve as guides and anchor points for the tendons and are stitched on the proximal, medial, and distal segments of each finger, and the proximal and distal components of the thumb. Each component was 3D-printed using flexible thermoplastic polyurethane (TPU) with a design intended to fit a men's medium glove size. The design also includes channels for polytetrafluoroethylene (PTFE) tendon guides and mounting features to anchor the tendons onto the dorsal and palmar side of the components.

The palm pads are made from 3D-printed TPU and are stitched onto the palm to serve as termination points for the PTFE Bowden tubing for each finger. The dorsal hand support was designed to hold the hand at a wrist extension angle of approximately 5 degrees, and is secured onto the device and hand through hook and loop straps contained in the palm guides. Fig. 2(a) shows the layout of the palm pads and Bowden tubing, while Fig. 2(b) shows the layout of the dorsal hand support.

B. Motor Assembly

The motor assembly is comprised of five motors to extend the fingers, five motors to flex the fingers, and several 3D-printed motor plates to secure the system in place on the user's forearm. These plates are mounted on the dorsal, palmar, and lateral sides of the arm. The plates on the dorsal side house motors for flexing and extending the index and pinky fingers, the plates on the lateral side house motors for flexing and extending the thumb, and the plates on the palmar side house motors for flexing and extending the middle and ring fingers. Fig. 3(a) shows a CAD model of the palmar motor assembly, noting the locations of each motor and pulley used to actuate the middle and ring finger tendon lines. Fig. 3(b) shows the assembly mounted on the palmar side of HEXOES, with the thumb assembly visible to the left.

The motors used for flexion are Faulhaber brushed DC motors with a 66:1 gear reduction rated at 193.9 mNm and 356.7 mNm of torque for continuous and intermittent operation, respectively, at a rated rotational output speed of 71 rpm (Micromo, Clearwater FL, USA). The output of the motor is transferred to a pulley with a diameter of 15.88 mm, resulting in an output of 26.1 N and 47.9 N of continuous and intermittent linear tendon force, respectively. The motors used for extension are Fitech FS60R Servo Motors, which can supply 148 mNm of stall torque and 130 max rpm. A pulley with a 15.88 mm diameter translates the torque output of the motor to 19.9 N of intermittent linear force and an estimated 10N of continuous force, allowing extension of the finger. The tendon line used is a braided high-strength filament which is run through 1/32" inner diameter PTFE tubing, and anchored to the finger components.

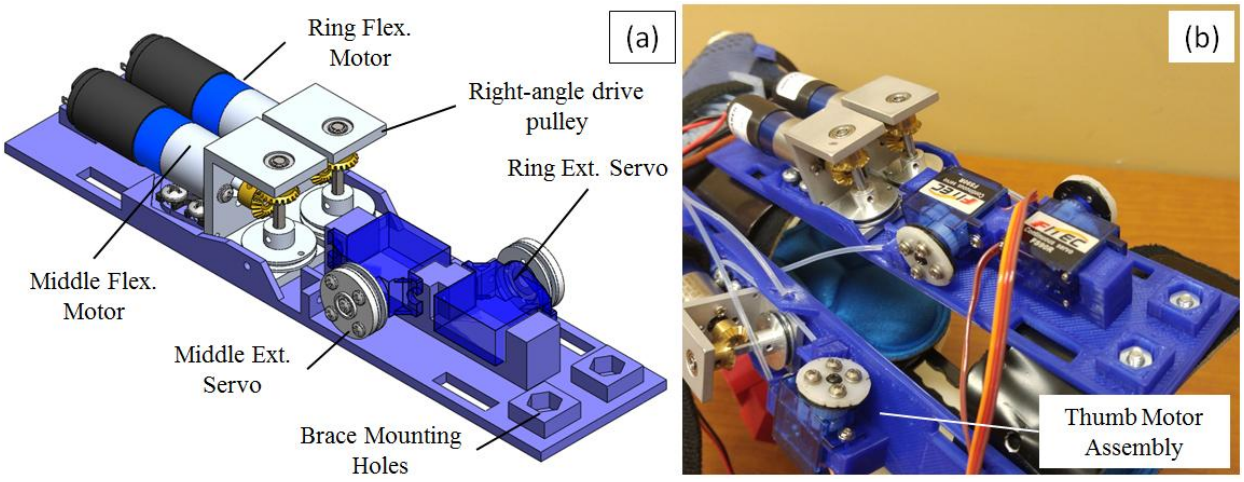

Figure 3. Isometric view of palmar motor assembly, containing middle and ring finger flexion and extension motors. An identical motor plate is mounted on the dorsal side of the forearm housing the index and pinky finger motors. A modified version which houses only the thumb flexion and extension motors is mounted on the lateral side of the arm. (b) Palmar motor assembly mounted on HEXOES.

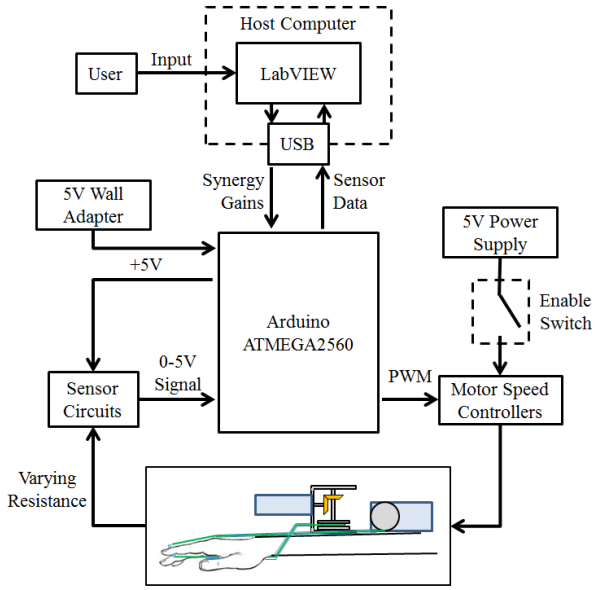

Figure 4. High-level physical architecture of HEXOES.

C. *Electrical System*

A high-level physical architecture of HEXOES is presented in Fig. 4. A computer running a LabVIEW program interfaces with the exoskeleton over a serial connection via USB. The LabVIEW program sends synergy gains derived from user input (button pressing, EMG/EEG activation, joystick manipulation, cursor movement, etc) to the exoskeleton. The microcontroller translates the low-dimensional synergy gains to 10 PWM signals which are output to motor speed controllers. A normally-off enable switch held by the user cuts power to the motors when released without removing power from the microcontroller. The motors actuate the user's fingers, which results in a change in the resistance of the flex sensors mounted in the glove. Voltage dividers using 35 kΩ resistors and a 5V signal from the microcontroller convert the varying resistance to a 0-5V signal which is digitized using the microcontroller's analog inputs. The voltage signals are converted to joint angles using a linear calibration, which will then be used in closed-loop control and returned to the host computer for recording.

III. Kinematic Characterization

A preliminary set of kinematic characteristics were measured using the on-board flex sensors with the exoskeleton placed on a mannequin arm with a 3D-printed articulated hand. Maximum powered range of motion and maximum joint angular velocity were measured for a range of motor powers along with positional accuracy. Ground-truth joint angles were measured using an iGaging 7" goniometer with a precision of 0.1 degrees and resolution of 0.05 degrees (Anytime Inc, Los Angeles, CA, USA). Sensor voltages were measured at 62.5 Hz.

Each of the 10 measured joints were calibrated by recording goniometer angles and voltages for three repetitions of each joint when the finger is in its neutral extended and its fully flexed position. A linear conversion for each joint using the average maximum and average minimum angles was calculated and used to convert voltages to angles.

Maximum joint angle and maximum angular velocity were recorded by independently flexing each finger from the neutral extended position until the flexion motor stalls, at which point the motor would be deactivated. Motors were run at various power settings, defined as percentages of motor power normalized to the active band of the motor. Examined power settings were 20, 40, 60, 80, and 100% power. Three repetitions were recorded for each motor power for each finger. Initial and final joint angles were measured by goniometer after each repetition of the 100% motor speed trials in order to assess the accuracy of the range of motion estimates. Sensor data was filtered using a third-order low pass Butterworth filter with a 1.5 Hz cutoff due to excessive motor noise. The end of each task was windowed to 1 second after maximum joint angle, which allowed the finger enough time to settle to its final flexion angle.

Table 1 shows the maximum angular velocity, in degrees/second, the maximum flexion angle, in degrees, and measured flexion angle, in degrees, for each joint in the 100% motor power repetitions. Mean and standard deviation are calculated across three repetitions. The sensors which showed excessive calibration error are omitted from the maximum angle and angular velocity dataset.

IV. Discussion

A. *Clinical Application*

The primary goal of HEXOES is to serve as a rehabilitative system capable of training subjects in the execution of synergy-based grasping motions. When viewed in the context of work done by [12] [13] [14], hand synergies appear to serve not only as a useful signal processing tool, but as a possible neural mechanism leveraged by the brain to control the highly complex hand. In the future HEXOES may offer a novel approach to rehabilitate patients with paralysis by training them in synergy-based movements that closely mirror how the brain naturally approaches motor control. Training patients in the building blocks of motion could improve their ability to more dexterously use their affected hand in addition to the strength and voluntary control gains offered by current practice. These improvements in stroke rehabilitation outcomes would lead to better quality of life and independence for stroke patients.

TABLE I. Kinematic Results of HEXOES (Mean ± SD).

Joint		Kinematic Variables		
		Max. Angular Velocity (°/s)	***Max. Calculated Flexion (°)***	***Measured Flexion (°)***
Thumb	MCP	106.5 ± 13.1	74.4 ± 8.6	32.7 ± 3.1
	PIP	-	-	60 ± 1
Index	MCP	-	-	44 ± 5.3
	PIP	-	-	36.7 ± 5
Middle	MCP	42.9 ± 16.1	46.2 ± 3.9	57.3 ± 1.2
	PIP	-	-	46.3 ± 3.8
Ring	MCP	134.1 ± 5.8	91.9 ± 3.6	71 ± 2.6
	PIP	135.8 ± 2.4	83.6 ± 3.4	34.7 ± 2.5
Pinky	MCP	-	-	41.7 ± 1.5
	PIP	13.4 ± 10.3	5.3 ± 1.9	22 ± 3.5

B. Design and Retrospective

The present design attempts to combine several techniques to reduce the size and weight of the exoskeleton. Soft wearable systems have been used in the past to produce biomimetic robotics, and tendon actuated mechanisms have been used successfully in the design of hand exoskeletons. The flexible 3D printed TPU finger and palm components are producible on professional or hobby-tier 3D printer, meaning that any patient who is outside of the optimal hand size range can have finger pieces quickly resized and reprinted.

Tendon-based actuation was chosen in order to minimize the weight of the hardware needed to transmit power from the motors to the fingers. Braided filament was chosen along with small-diameter, low-friction PTFE tubing to compose of a Bowden tube system with adequate strength and minimal weight. A Bowden system has the advantage of structurally decoupling the hand assembly from the motor assembly, allowing the motors to be located remotely from the forearm. However, extending the length of the Bowden tubing increases line friction, and extended unsupported lengths of tubing are susceptible to deformation under load which could seize the tendon. These problems may be addressed by selecting tubing with larger wall thickness, but the added stiffness of the tubing may be too cumbersome and frustrating for a patient to wear. Extensive work has been done by the SNU lab to manage issues of tensioning and unspooling that are also associated with such systems [15].

A redesigned, compliant tendon driven system will enable ten DoF actuation of the MCP and PIP/IP of each finger and thumb while resolving some spooling issues without the additional weight of extra motors. The mounting hardware can also be redesigned to remove the orthopedic brace, thus reducing the weight of the system significantly. This is important as the current size and weight of the exoskeleton would make donning and doffing the glove difficult.

Table 1 omitted sensors which did not maintain a valid calibration during characterization. Sensor placement on the glove was sub-optimal for some of the affected sensors with respect to the actual rotation axis of the mannequin hand. Improved sensor circuits may also be employed in future revisions, such as the impedance buffer circuit presented by [16] [17]. Optical isolation between the microcontroller and the motor circuits would also eliminate noise from the operation of the motors, such as in [18]. With these mechanical changes and sensor system improvements, a closed-loop synergy controller can properly be implemented and tested with healthy subjects and stroke patients.

V. Conclusion

The design of a novel tendon-driven soft hand exoskeleton with 5 actuated DoF is presented along with preliminary data on kinematic performance using a mannequin hand. Accuracy results indicate that additional development needs to be done to refine the joint angle measurement system before closed-loop control can be implemented. Range of motion and estimates on joint angle velocities indicate that the mechanical design is adequate to move forward, with future design improvements also outlined. The biomechanical implications of kinematic synergies along with clinical applications of a synergy-driven exoskeleton are discussed.

Acknowledgment

The authors would like to acknowledge the Biomedical engineering, Chemistry, and Biological Sciences department at Stevens Institute of Technology as well as the Center for Healthcare Innovation for their continued support of our research. The authors would also like to thank Dr. Kishore Pochiraju and the Stevens Mechanical Engineering Department for feedback on the design of HEXOES, as well as Dr. Michael Majsak for clinical input.

References

[1] Butefisch C, Hummelsheim H, Denzler P, Mauritz K H. Repetitive training of isolated movements improves the outcome of motor rehabilitation of the centrally paretic hand. Journal of the neurological sciences; 1995;130(1):59–68.

[2] Carey J R, Durfee W K, Bhatt E, Nagpal A, Weinstein S A, Anderson K M, et al. Comparison of finger tracking versus simple movement training via telerehabilitation to alter hand function and cortical reorganization after stroke. Neurorehabilitation and neural repair; 2007;21(3):216–232.

[3] Lo A C, Guarino P D, Richards L G, Haselkorn J K, Wittenberg G F, Federman D G, et al. Robot-assisted therapy for long-term upper-limb impairment after stroke. New England Journal of Medicine; 2010;362(19):1772–1783.

[4] Lum P S, Godfrey S B, Brokaw E B, Holley R J, Nichols D. Robotic approaches for rehabilitation of hand function after stroke. American journal of physical medicine & rehabilitation; 2012;91(11):S242-S254.

[5] Schabowsky C N, Godfrey S B, Holley R J, Lum P S. Development and pilot testing of HEXORR: hand EXOskeleton rehabilitation robot. Journal of neuroengineering and rehabilitation; 2010;7(1):1.

[6] Takahashi C D, Der-Yeghiaian L, Le V, Motiwala R R, Cramer S C. Robot-based hand motor therapy after stroke. Brain; 2008;131(2):425–437.

[7] Koeneman E J, Schultz R S, Wolf S L, Herring D E, Koeneman J B. A pneumatic muscle hand therapy device. Engineering in Medicine and Biology Society, 2004. IEMBS'04. 26th Annual International Conference of the IEEE; 2004;1:2711–2713.

[8] Lucas L, DiCicco M, Matsuoka Y. An EMG-controlled hand exoskeleton for natural pinching. Journal of Robotics and Mechatronics; 2004;16:482–488.

[9] Ho N S K, Tong K Y, Hu X L, Fung K L, Wei X J, Rong W, et al. An EMG-driven exoskeleton hand robotic training device on chronic stroke subjects: Task training system for stroke rehabilitation. 2011 IEEE international conference on rehabilitation robotics; 2011:1–5.

[10] Matrone G C, Cipriani C, Carrozza M, Magenes G. Real-time myoelectric control of a multi-fingered hand prosthesis using principal components analysis. Journal of neuroengineering and rehabilitation; 2012;9(1):40.

[11] Brooks V B. Motor control. How posture and movements are governed. Physical therapy; 1983;63(5):664–673.

[12] Brooks V B. The neural basis of motor control. New York: Oxford University Press; 1986.

[13] Santello M, Baud-Bovy G, Jörntell H. Neural bases of hand synergies. Frontiers in Computational Neuroscience; 2013;7.

[14] In H, Kang S, Cho K-J. Capstan brake: Passive brake for tendon-driven mechanism. 2012 IEEE/RSJ International Conference on Intelligent Robots and Systems; 2012:2301–2306.

[15] Ahmed S F, Ali S M B, Qureshi S M. Electronic Speaking Glove for Speechless Patient. Sustainable Utilization and Development in Engineering and Technology (STUDENT); 2010:56–60.

[16] Syed A, Agasbal Z T H, Melligeri T, Gudur B. Flex Sensor Based Robotic Arm Controller Using Micro Controller. Journal of Software Engineering and Applications; 2012;5:364–366.

[17] Syed A, Agasbal Z T H, Melligeri T, Gudur B. Flex Sensor Based Robotic Arm Controller Using Micro Controller. Journal of Software Engineering and Applications; 2012;5:364–366.

View publication stats